Crystallographic texture for tube and plate of the superelastic/shape-memory alloy Nitinol used for endovascular stents

S. W. Robertson,[1] V. Imbeni,[2] H.-R. Wenk,[3] R. O. Ritchie[1]
[1]*Department of Materials Science and Engineering, University of California, Berkeley, California 94720*
[2]*SRI International, Menlo Park, California 94025*
[3]*Department of Earth and Planetary Science, University of California, Berkeley, California 94720*

Received 4 June 2004; revised 23 August 2004; accepted 25 August 2004
Published online 14 December 2004 in Wiley InterScience (www.interscience.wiley.com). DOI: 10.1002/jbm.a.30214

Abstract: The superelastic/shape-memory material, Nitinol, an approximately equiatomic alloy of Ni and Ti, is rapidly becoming one of the most important metallic implant materials in the biomedical industry, in particular for the manufacture of endovascular stents. As such stents are invariably laser-machined from Nitinol tubes or sheets rolled into tubes, it is important to fully understand the physical phenomena that may affect the mechanical behavior of this material. With tubing and plate, one major issue is crystallographic texture, which can play a key role in influencing the mechanical properties of Nitinol. In this article, we present a study on how geometry and heat treatment can affect the texture of Nitinol, with specific quantification of the texture of Nitinol tube used for the production of endovascular stents. © 2004 Wiley Periodicals, Inc. J Biomed Mater Res 72A: 190–199, 2005

Key words: Nitinol; texture; stents

INTRODUCTION

Nitinol, a nearly equiatomic nickel–titanium alloy known for its shape memory, superelastic properties, and biocompatibility, has proved particularly successful in biomedical applications, including endovascular stents, vena cava filters, dental files, and guidewires for noninvasive surgery. Both superelasticity and shape memory are associated with a stress- or temperature-induced phase transformation of its crystalline structure.

When conventional engineering materials (like stainless steel) are mechanically loaded, they undergo elastic deformation (which is completely recoverable), followed by plastic deformation (which is permanent), and ultimately fail. Nitinol responds differently: its elastic response is followed by a stress-induced phase transformation from a cubic (austenite) phase to an orthorhombic (R-phase) to a monoclinic (martensite) phase[1] that can result in fully recoverable macroscopic strains as high as 8% or more. On unloading, the martensite becomes unstable and transforms back to austenite, with a concomitant macroscopic strain recovery.

Nitinol exhibits superelasticity over a temperature range compatible with body temperature,[2,3] and has generally good corrosion resistance in physiological environments. It has been widely adopted in the medical community as physicians seek to use fewer invasive procedures in order to reduce unnecessary patient trauma. These procedures require instruments and devices that can pass through small openings and then elastically spring back into the desired shapes. Nitinol has a flexibility that is 10 to 20 times greater than that of stainless steel and has a biocompatibility close to titanium, and is thus being widely used to fabricate self-expanding cardiovascular stents. Although the superelastic and shape-memory properties are ideally suited for such biomedical applications, they add substantial complexity to the design and modeling of Nitinol devices.

The production of Nitinol biomedical devices can involve several processing procedures, such as tube drawing, plate rolling, and heat treatment, in order to modify microstructure, transformation temperatures, and mechanical properties. These procedures can lead to texturing (crystallographic alignment) of the material. Because Nitinol derives its unique nonlinear and anisotropic mechanical behavior from stress-induced

Correspondence to: R. O. Ritchie; e-mail: roritchie@lbl.gov
Contract grant sponsor: Nitinol Devices and Components, Inc.
Contract grant sponsor: National Science Foundation; contract grant number: CMS-0409294

martensitic transformations, where the resulting strains are affected by crystallographic orientation, it is clear that texture can have a marked influence on its mechanical properties. However, there have only been a few, mainly qualitative, studies on texture in Nitinol sheets and plates[4–11] and no corresponding information for Nitinol tubes, the starting material for many endovascular stents.

Of the work that has been performed, Gall and Sehitoglu[12] concluded that texture, and consequently the martensite variants active during the transformation, are the source of the compression–tension asymmetry of Nitinol. Furthermore, Vaidyanathan and colleagues[13] suggest that texturing can occur in Nitinol when martensite is stress-induced from austenite via such compression loading. That texture may also be responsible for the anisotropy in the mechanical behavior of Nitinol in tension and torsion, as demonstrated by McNaney and colleagues.[14]

Accordingly, it is the objective of the present study to seek further understanding of how processing and heat treatment can affect the texture in Nitinol, specifically by quantifying the texture of drawn tubes in comparison to rolled plates. The motivation for this comparison is to provide the first characterization of the texture of the Nitinol tubes that are used in the fabrication of many stent devices, and to determine if such tubes can be simply modeled as plates rolled into a cylindrical form. The latter can be important where the flat geometry of plate specimens is preferred over a curved geometry for certain testing conditions, such as for microscopy studies which require a flat surface for resolution.

EXPERIMENTAL PROCEDURES

Nitinol (50.8 at. % Ni, 49.2 at. % Ti) in the form of both tubing and plate was received from Nitinol Devices & Components, Inc. (NDC, Fremont, CA); the tube dimensions were 4.6 mm outer diameter and 3.9 mm inner diameter, whereas the plate sections were 15 mm square by 1 mm thick. The sample geometries (tube vs plate) were chosen to determine if the processing (drawing vs rolling) and general geometric constraint has a significant effect on the texture. The as-processed structures were further compared to corresponding annealed structures; specifically, the following conditions were examined:

- *as-drawn or as-rolled condition:* as-drawn tube or as-rolled plate was reheated for 5 min at 485°C in an air furnace, followed by an ice-water quench. Although this is not truly an as-drawn/rolled condition, we use this label because the heat treatment is relatively mild and serves only to stress relieve and slightly lower the tensile strength.

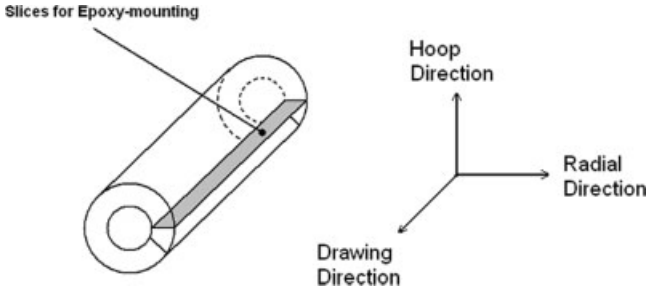

Figure 1. Schematic diagram of slices from tube taken for texture measurements.

- *annealed condition:* as-drawn/rolled Nitinol was annealed *in vacuo* at 850°C for 30 min followed by a slow cool of −10°C per min. This heat treatment does not fully normalize the microstructure, but is used here as it represents a typical industry anneal.

Textures were measured at room temperature with an X-ray pole figure goniometer, as samples were too deformed (from the prior processing) for scanning electron microscopy–electron backscatter probe measurements. To provide large enough flat samples, the tube was sliced into sections, as shown in Figure 1; the sections were then lined up side-by-side, cold-mounted in epoxy, and polished flat. After combining the multiple tube slices into two samples (as-drawn and annealed), their sizes were approximately 10-mm square, which is the minimum sample size for quantitative texture analysis with an X-ray pole figure goniometer in reflection geometry. All samples were mechanically ground and polished to a 0.05μm finish to permit optimal reflective X-ray diffraction and establish consistency among the samples.

Optical micrographs of the microstructures are shown in Figure 2. All samples were heated to approximately 50°C prior to testing, and were maintained above the austenite finish temperature, A_f, temperature to ensure they were fully austenitic throughout the test. The micrographs show martensitic grains in the as-drawn/rolled samples; however, these are polishing artifacts as the stresses from grinding and polishing cause transformation in the exposed grains which leaves residual surface relief on etching. Moreover, the apparent grain sizes of ~20 μm observed with optical microscopy for the as-drawn conditions in Figure 2(a,c) also give a false impression; the actual grain sizes are much smaller, specifically on a submicrometer scale, and can only be revealed by transmission electron microscopy, as shown in Figure 3(a). Table I gives a list of properties for the four Nitinol sample types that were analyzed in this study.

Pole figures were measured with a Huber X-ray pole figure goniometer, with Cu-Kα radiation

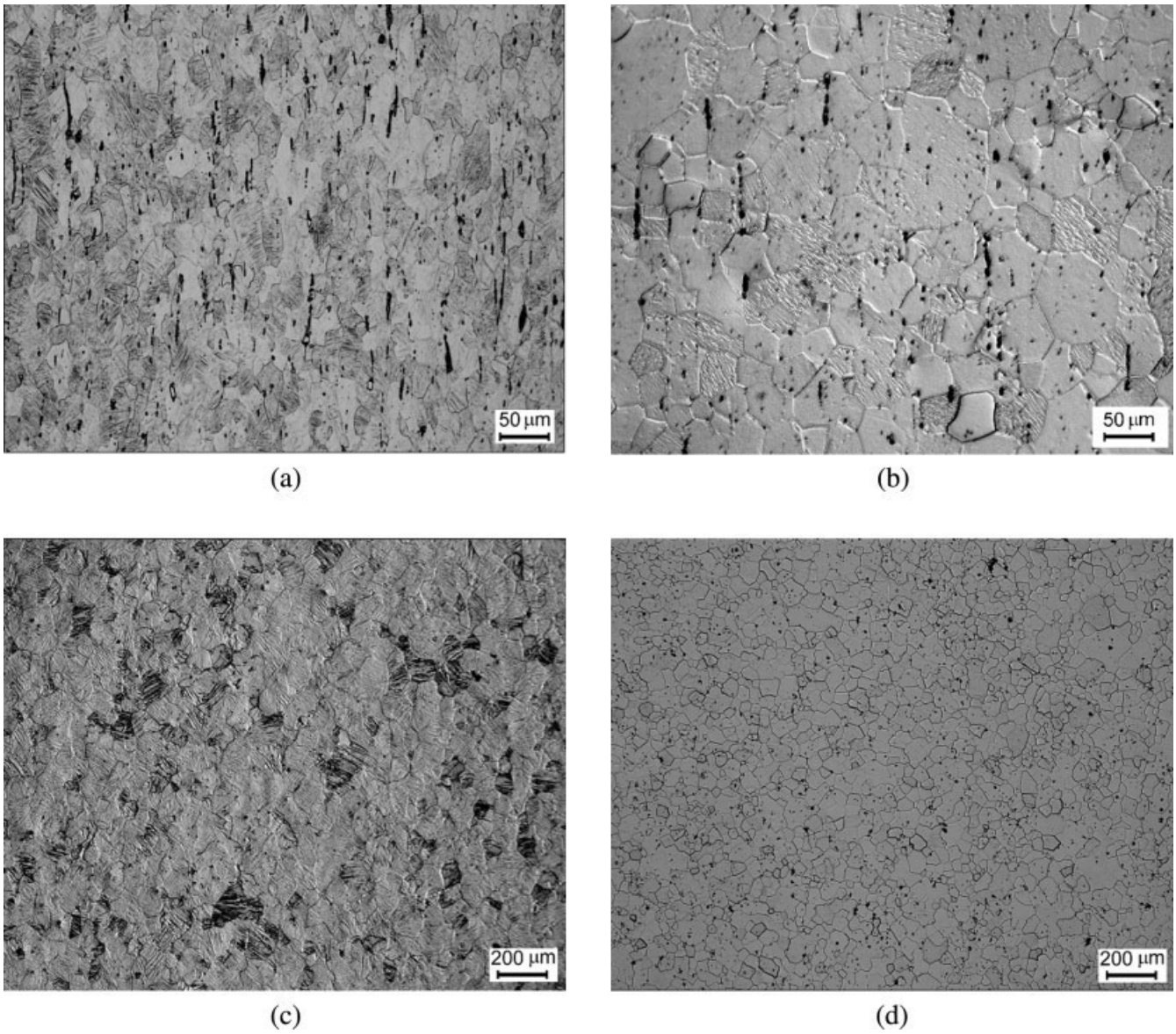

Figure 2. Optical micrographs of the microstructure of the (a) as-drawn tube, (b) annealed tube, (c) as-rolled plate, and (d) annealed plate. Etchant: 3.2% HF, 14.6% HNO_3, balance deionized water. The drawing/rolling direction is vertical in each micrograph.

source at 40 kV and 14 mA, and a graphite monochromator. The crystallographic texture of the Nitinol was determined from three incomplete measured pole figures, namely the 110, 200, and 211 poles, at θ values of, respectively, 21.3°, 30.8°, and 38.9° for Cu-Kα radiation, where θ is half of the angle between the X-ray source and the detector. The raw intensities were corrected for background and defocusing and only data out to a maximum pole distance of 65° were used. The Williams–Imhof–Matthies–Vinel (WIMV)[15] algorithm, which calculates orientation distributions from pole figures, was used in the BEARTEX software package for quantitative texture analysis in order to obtain the orientation distribution functions (ODF).[16] From the ODF, pole figures for 100, 110 and 111 were recalculated following standard smoothing and rotation operations. The smoothing operation was performed mainly to reduce the effects (if any) of highly oriented single crystals in the bulk sample. Rotation was necessary to orient each pole figure in the same reference orientation for comparison among the samples. The experimental pole figures and inverse pole figures for Nitinol tube presented in this article represent the average of three separate tests. For the Nitinol plate, only one test was used in the texture analysis because of limited sample supply; however, the Nitinol plate texture has been characterized previously in the literature[4–7] and the current results were found to conform closely to these prior data.

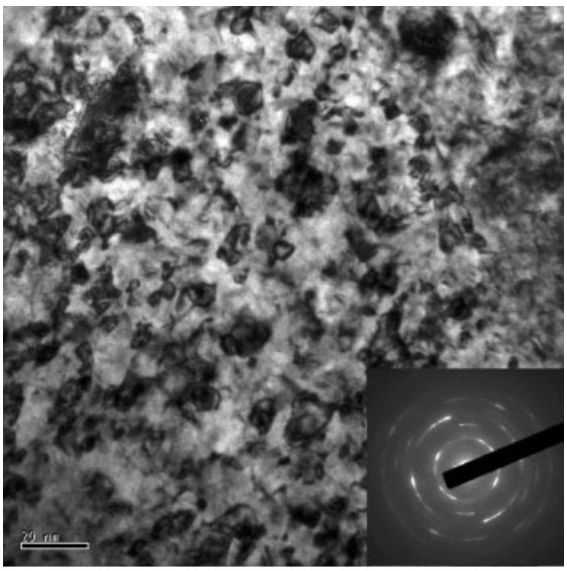

(a)

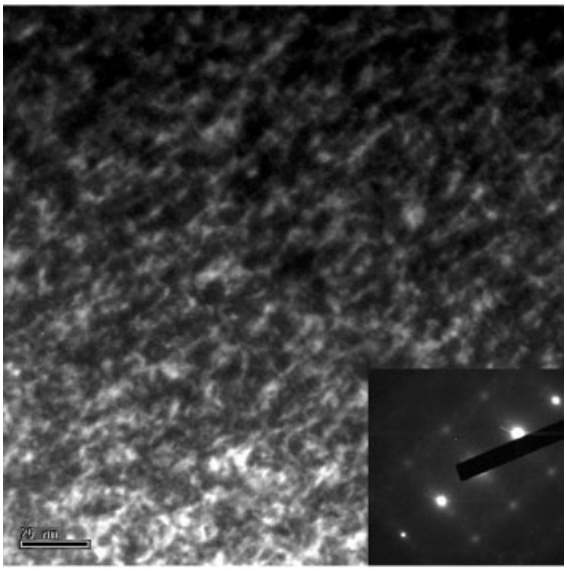

(b)

Figure 3. Transmission electron micrographs of the microstructure of the (a) as-drawn tube, showing a subgrain microstructure and diffraction pattern that reveals texture, and (b) annealed tube with residual dislocations but a localized single crystal diffraction pattern; [100] zone axis.

RESULTS AND DISCUSSION

Pole figures

The pole figures for the Nitinol tube and plate in the as-drawn/rolled and annealed conditions are shown in Figure 4. It is clear that the nature and degree of texture is different in all four conditions. Particularly interesting is the fact that all four conditions show marked texture; indeed, especially the annealed samples which have a stronger texture intensity (i.e., more red regions) than the as-drawn/rolled samples.

With respect to the as-drawn tube [Fig. 4(a)], the main feature is a maximum in the 111 pole figure in the hoop direction, as indicated by the yellow regions at 6 and 12 o'clock. There is also a strong maximum in the 111 pole figure parallel to the radial direction. In addition, texture minima occur in the 100 pole figure parallel to all three primary directions (drawing, hoop, and radial), as indicated by white areas in Figure 4(a) at 3 and 9 o'clock, 6 and 12 o'clock, and center, respectively. A strong texture maximum is apparent at 45° from each of the principal axes in the 100 pole figure.

The annealed tube, shown in Figure 4(b), contains 111 texture maxima in the hoop and radial directions, as did the as-drawn tube. Also similar to the as-drawn tube, the annealed tube shows a 100 texture maximum oriented 45° to the three principal axes. However, unlike the as-drawn tube, the strongest 100 texture maximum is between the radial and hoop directions. The 110 texture in the annealed tube is quite different from that in the as-drawn tube. The texture maximum is between the radial and drawing directions as indicated by the two yellow regions near the center of the 110 pole figure [Fig. 4(b)], and there is also a weak trend to the hoop and drawing directions, as indicated by green regions at 12 and 3 o'clock, respectively.

The as-rolled plate displays a 110 maximum in the rolling direction, as indicated by the highest intensity at 3 and 9 o'clock [Fig. 4(c)]. Also, there is a 111 maximum parallel to the normal direction, as shown by the red region at the center of Figure 4(c). Furthermore, the as-rolled plate has texture minima for 100

TABLE I
Various Crystallographic and Thermodynamic Properties of the Studied Nitinol Tube and Plate

	Transformation Temperatures,* °C					
Condition	M_s	M_f	A_s	A_f	R-Phase Present?	Average Grain Size
Tube						
As-drawn	22	8	16	28	Yes	10 nm
Annealed	0	−25	−8	4	Yes	40 μm
Plate						
As-drawn	25	3	13	30	Yes	10 nm
Annealed	−6	−30	−7	−4	Yes	75 μm

*Determined by differential scanning calorimetry (tangent intercept method). M_s, M_f and A_s, A_f are, respectively, the martensite and austenite start and finish temperatures.

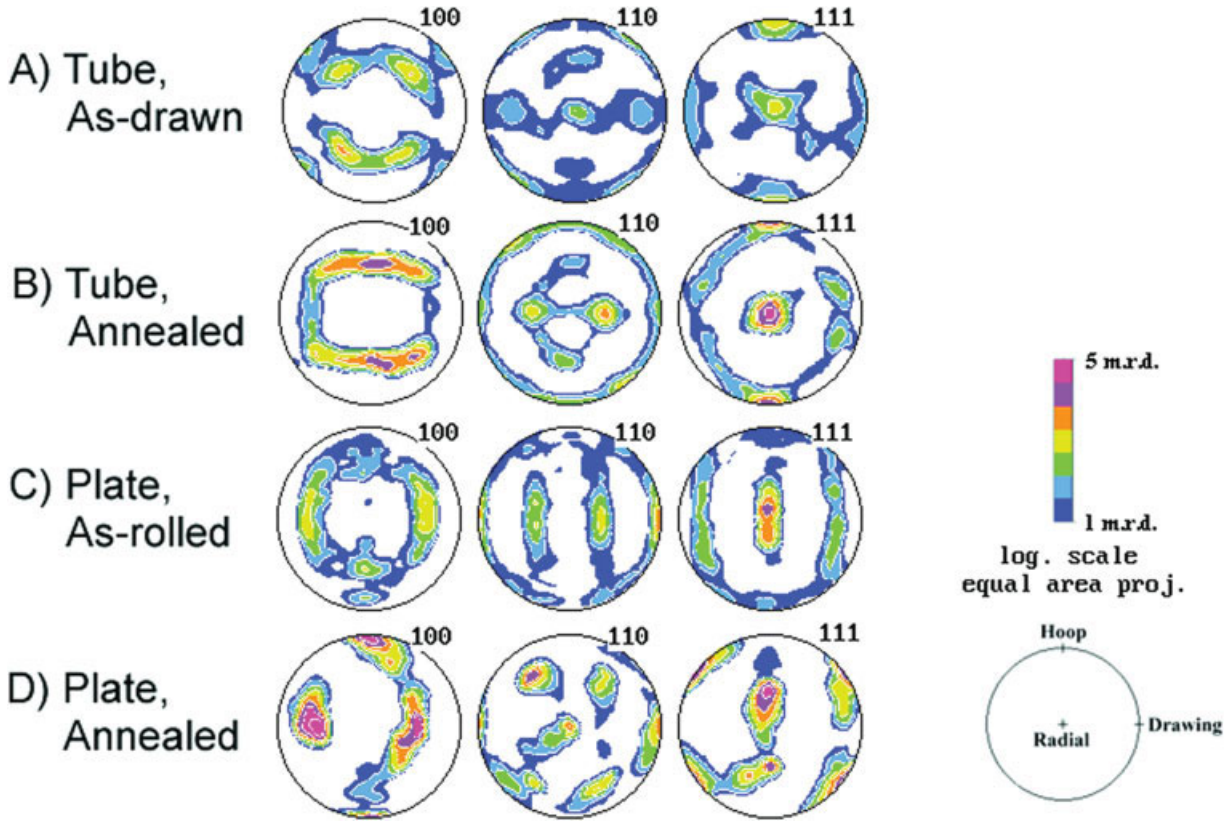

Figure 4. 100, 110, and 111 pole figures showing texture in the (a) as-drawn tube, (b) annealed tube, (c) as-rolled plate, and (d) annealed plate.

and 111 poles parallel to the rolling direction, as indicated by white areas at 3 and 9 o'clock in Figure 4(c). Another minimum was observed in the 110 pole figure parallel to the normal (thickness) direction, as indicated by the white area in the center of Figure 4(c). Lastly, there are local texture concentrations in the 100, 110, and 111 pole figures located between all three of the principal axes. The pole figures for this plate are similar to other body-centered cubic (bcc) rolling textures.[17]

Pole figures of the annealed samples clearly show the strongest texture intensities indicating that the material is still highly textured following heat treatment. There are some, albeit few, similarities between the annealed and as-drawn plate textures. Both exhibit strong 110 maxima in the rolling direction, and 111 maxima in the normal direction. However, the annealed plate shows a strong 100 maximum in the transverse direction and 111 maxima approximately 45° between the rolling and transverse directions [e.g., red region at 2 o'clock in Fig. 4(d)].

These results provide the first evidence that the texture in Nitinol tube is quite different to that in plate. The only apparent similarity between Nitinol tube and plate texture is the 100 minimum in the rolling/drawing direction, and the strong 111 maximum in the radial/normal direction. These significant differences in texture indicate that for testing and evaluation purposes, plate should not be used as a substitute for tubes when samples are geometry limited. Moreover, it is clear that plates that have been folded into a cylinder cannot be assumed to have the same texture as actual tubes.

The current results on Nitinol plate textures compare favorably with those reported in the literature[4,5,7]; however, to our knowledge there are no previous reports on the tube textures for comparison to the current results. Specifically, the plate textures in Figure 4(c) are similar to those determined previously by Monasevich and colleagues,[4] Li and colleagues,[5] and Inoue and colleagues[7] on other Nitinol plate and sheet geometries. However, pole figures derived by Kitamura and colleagues[8] were different from those obtained in the present study. Their work was focused on much thinner (100 μm) Nitinol sheet and revealed a texture maximum of the 110 pole normal to the sheet, in contrast to the present data where a texture minimum is found at that location in the as-drawn condition, and only a slight tendency to that texture in the annealed plate. Furthermore, they observed that with higher temperature heat treatments (400°C vs 600°C for 1 h), the maximum intensities of the 110 concentrations in the rolling direction had a diffuse extension toward the transverse direction, creating local maxima.

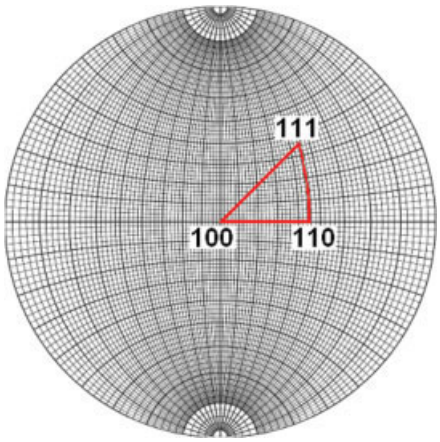

Figure 5. [100] Wulff net stereographic projection showing the segment viewed in the inverse pole figures. [Color figure can be viewed in the online issue, which is available at www.interscience.wiley.com.]

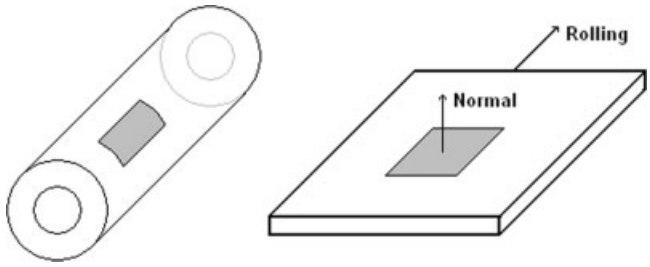

Figure 7. Diagram of the orientation of the crystallographic planes which are can be derived from the radial/normal pole directions given by the inverse pole figures in Figure 6.

Inverse pole figures

In light of materials scientists' familiarity with stereographic projections (Wulff nets) of crystal directions, it is perhaps more illuminating to visualize texture using inverse pole figures (IPF), which are representations of a sample direction relative to crystal coordinates and are calculated from the ODF. Figure 5 shows the section of the stereographic projection that is used in the inverse pole figures. Using these procedures, inverse pole figures for the annealed and as-rolled/drawn tube and plate are given in Figure 6. This figure plots pole distributions in the radial/normal direction (leftmost IPF) and in the drawing/rolling direction (rightmost IPF). Although the radial/normal IPFs represent pole directions, because of cubic symmetry they can also describe a plane which is parallel to the rolling direction; see Figure 7 for a graphical representation of these planes. The texture described in the following section is in the form {hkl}⟨uvw⟩, where {hkl} is the crystallographic plane oriented parallel to the rolling direction (or alternatively the pole oriented radially as discussed above), and ⟨uvw⟩ is the crystallographic direction vector which is parallel to the rolling direction. The intensity of such plane and direction pairs is calculated from texture analysis and is presented in wt % in Table II.

Drawing direction orientations in the as-drawn tube

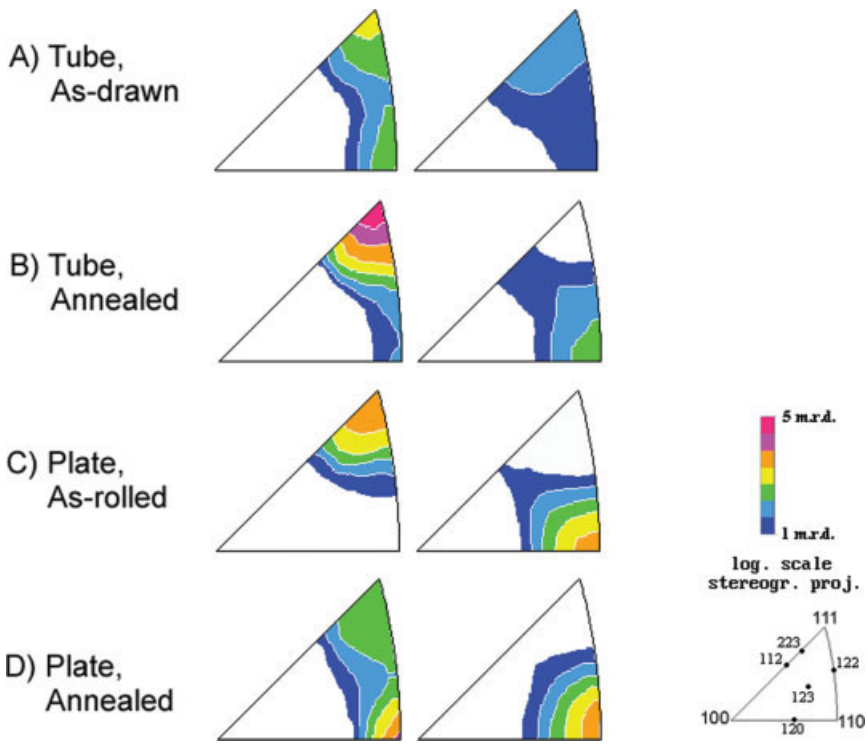

Figure 6. Inverse pole figures showing the radial/normal direction (left) and drawing/rolling direction (right) crystallographic populations for the (a) as-drawn tube, (b) annealed tube, (c) as-rolled plate, and (d) annealed plate.

TABLE II
Quantified Texture Component-Weight (in-percentage)

Condition	Component	Euler Angle†, Degrees α	β	γ	Radius, Degrees (Δβ)	Miller Index {hk1}⟨uvw⟩	Wt %
Tube, As-Drawn	1	45	45	0	20	{110}⟨223⟩*[1]	26
	2	30	56	45	15	{111}⟨110⟩	10
	3	0	57	45	10	{111}⟨112⟩	4
Tube, Annealed	1	45	58	45	12	{111}⟨123⟩	20
	2	55	45	0	15	{110}⟨112⟩	10
	3	90	45	45	10	{223}⟨110⟩	8
	4	275	40	25	10	{123}⟨120⟩	5
Plate, As-Drawn	1	60	45	45	15	{111}⟨112⟩	15
	2	270	45	45	15	{223}⟨110⟩*[2]	13
	3	270	75	45	15	{122}⟨110⟩	11
Plate, Annealed	1	313	45	35	25	{435}⟨312⟩	45
	2	0	45	0	20	{110}⟨110⟩	30

*Because of the close proximity of certain crystallographic orientations on a stereographic projection, the following orientations could not be excluded: (1) {110}⟨334⟩ or {110}⟨557⟩, and (2) {334}⟨110⟩ or {557}⟨110⟩. Due to the high symmetry of the simple cubic structure, the lower ordered orientations (presented in the table) are most likely the correct identification.
†Angles defined in Figure 8.

[Fig. 6(a)] are relatively delocalized; this is also apparent when quantifying the texture (see discussion below). The primary texture in the drawing direction forms a ring containing the ⟨223⟩ and ⟨110⟩ direction families. The radial poles, and thus planes parallel to the drawing direction, were primarily 111 and 110 type.

Annealed tubes have strong 111 type and nearby crystallographic radial direction textures [Fig. 6(b)]. The drawing directions are more defined in the annealed tubes than the as-drawn tubes, and show a maximum near ⟨110⟩. However, the drawing directions are distributed over a range of orientations including ⟨123⟩, ⟨112⟩, and ⟨120⟩, as discussed in the next section where the results are quantified.

The as-rolled plate inverse pole figures show a strong tendency of ⟨110⟩ texture in the rolling directions [Fig. 6(c)] with broadening similar to the annealed tube texture. For the normal direction there are strong maxima near 111, with broadening towards 223 and 122.

Figure 6(d) shows that, following annealing, the plate normal direction significantly shifts from the 111 position in the as-drawn condition toward 110. In addition, the rolling direction is much more centered about ⟨110⟩.

Crystal orientation distribution (COD)

The relative weight of each orientation component in the samples was quantified by making use of crystal orientation distribution (COD) sections.[18] Because of cubic crystal symmetry for austenitic Nitinol, only COD sections through γ = 45° were needed for a complete component analysis which is accomplished by a simple addition of component intensities from the ODF (see Fig. 8 for Euler angle convention). To determine the component weight percentages, the center of each component was described by a triplet of Euler angles around the strongest orientation concentrations on the COD maps. Next, the edge of each component was described by another Euler triplet by holding α and γ constant such the radius could be defined in terms of Δβ (Table II). Using the center and radius, a sphere was defined around each component which was subtracted from the ODF using BEARTEX quan-

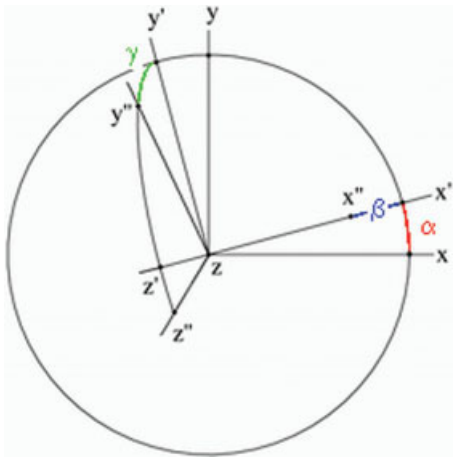

Figure 8. Euler angles (Roe/Matthies convention) defined around the sample axes (x = drawing, y = circumferential, z = radial); α is the angle formed when the x axis is rotated to x' around z; β is the angle between x' and x'' as the x' axis is rotated around y'; γ is the angle between y' and y'' (or z' and z'') formed when the $y'z'$ plane is rotated around x''. [Color figure can be viewed in the online issue, which is available at www.interscience.wiley.com.]

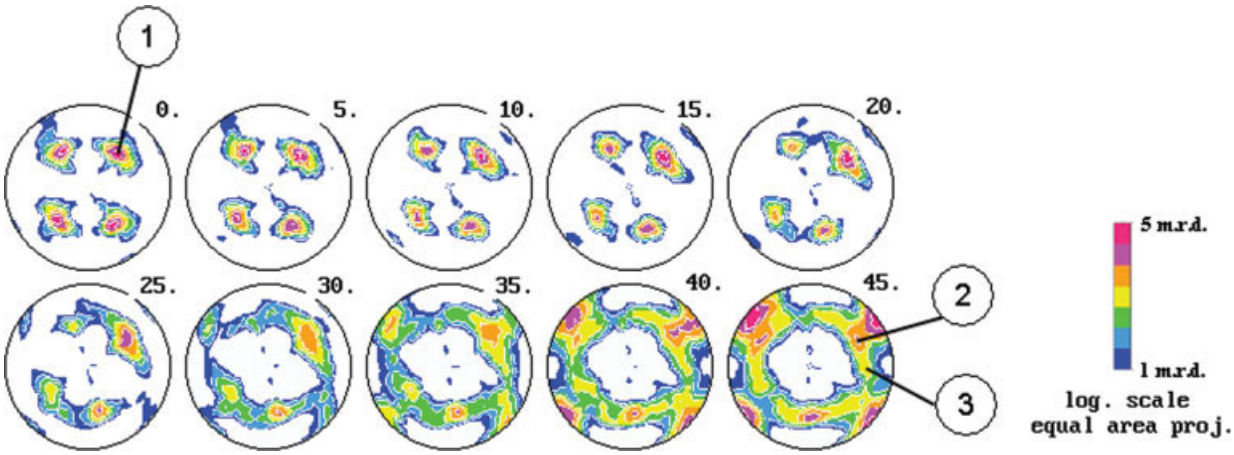

Figure 9. As-drawn tube crystal orientation distribution in 5° Euler γ space increments. Note the principal component locations which are labeled 1–3. See Table II for quantification of these principal components.

tification software. The quantification algorithm recorded how many orientations fell into each sphere and compared that value with all orientations to arrive at a component weight percentage. Positions [in Euler angles and {hkl}⟨uvw⟩ description], sphere radius, and orientation volume (in percentage) are listed in Table II.

Crystal orientation distribution plots are provided as reference in Figures 9 through 12, with the corresponding quantified component volumes shown in Table II. Only textures representing 4% or more of the total volume are tabulated. Just as with the pole figures, the CODs of the as-drawn and annealed tube appear reasonably similar. However, slight shifts in the texture resulted from the annealing process and are apparent when quantified (see Table II). Specifically, the {110}⟨223⟩ dominant texture in the as-drawn tube (component 1, Fig. 9) reoriented into a {110}⟨112⟩ in the annealed condition (component 2, Fig. 10). In addition, the {111}⟨110⟩ (Fig. 9, component 2) rotated into a {111}⟨123⟩ configuration and became the preferred orientation upon annealing. These quantified results demonstrate that although the texture remains similar, heat treatment clearly has an effect on modifying the crystallographic texture of Nitinol tube.

The plate CODs appear entirely different between the as-drawn and annealed condition indicating a widely different texture following the heat treatment. Whereas the as-rolled plate contained an evenly distributed texture among three components ({111}⟨112⟩, {223}⟨110⟩, and {122}⟨110⟩), which represented only 40% of the total volume, the annealed plate showed that the 75% of the crystallites are oriented in one of only two orientations, either {435}⟨312⟩* or the {110}⟨110⟩, perhaps from grain-growth and/or recrystallization.

CLOSING REMARKS

Because Nitinol depends on coordinated atomic movements for phase transformations, which defines

*This plane/direction pair is not perfectly co-planar, but represents the approximate low-index description.

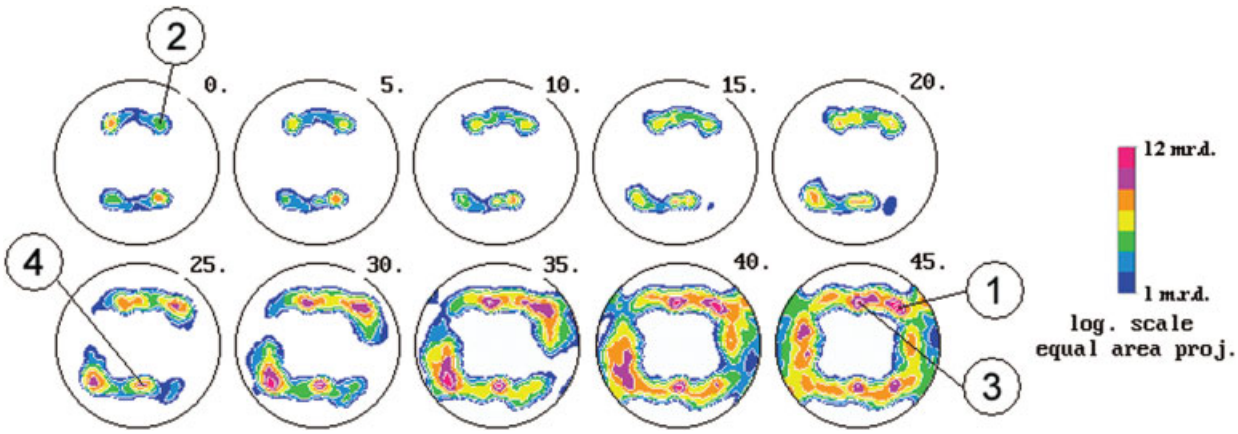

Figure 10. Annealed tube crystal orientation distribution in 5° Euler γ space increments. Note the principal component locations which are labeled 1–4. See Table II for quantification of these principal components.

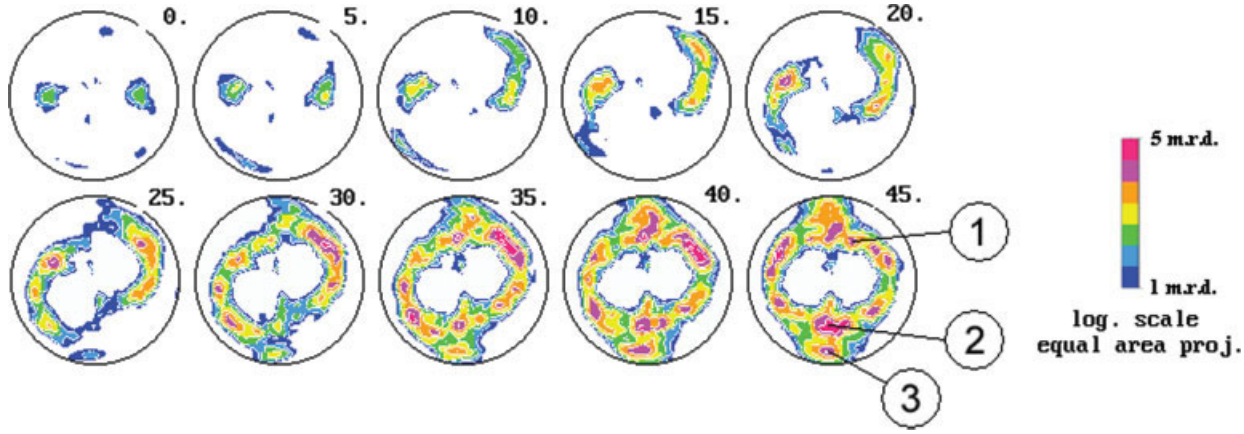

Figure 11. As-rolled plate crystal orientation distribution in 5° Euler γ space increments. Note the principal component locations which are labeled 1–3. See Table II for quantification of these principal components.

its unique mechanical behavior, any significant alignment of the atomic planes from texture in the polycrystalline material can have a marked influence on the mechanical response by either limiting or promoting that phase transformation. Previous work has shown that in sheet or bar Nitinol, nearly all mechanical properties are influenced by the texture. Gao and Yi[19] demonstrated the marked influence of texture on the tensile Young's modulus, transformation stress and transformation strain. Other studies by Gall and Sehitoglu,[12] and McNaney and colleagues,[14] suggest that the anisotropy associated with various loading conditions (tension, compression, and torsion) can also be attributed to the texture of polycrystalline Nitinol. Interestingly, Yuan and Yi[20] show that the experimentally observed tensile stress–strain response can be accurately predicted, through the Taylor factor, from theoretical strains obtained through inverse pole figure data.

Although some studies have been performed which quantify the texture of Nitinol plate and rod, to our knowledge this work is the first to quantify the texture of Nitinol tubing. This is of importance to the biomedical companies who use Nitinol tubes as the starting material for their products, for example, endovascular stents, as the tube has very different texture than other Nitinol product forms, such as sheet and rod; moreover, it differs from the expected α-⟨110⟩ fiber texture parallel to the rolling direction and γ-[111] fiber texture parallel to the normal direction of rolled body-centered-cubic materials.[17] Additionally, it is clear that high-temperature annealing has little effect in Nitinol in removing this texture.

CONCLUSION

Austenitic Nitinol tube and plate (0.35 mm wall thickness and 1 mm thick, respectively) have been shown to be highly susceptible to crystallographic texturing following mechanical processing (drawing or rolling) and heat treatment. As-drawn Nitinol tubes, which are the starting material for the fabrication of many endovascular stents, have a preferred orientation of {110}⟨223⟩ representing 26% of the com-

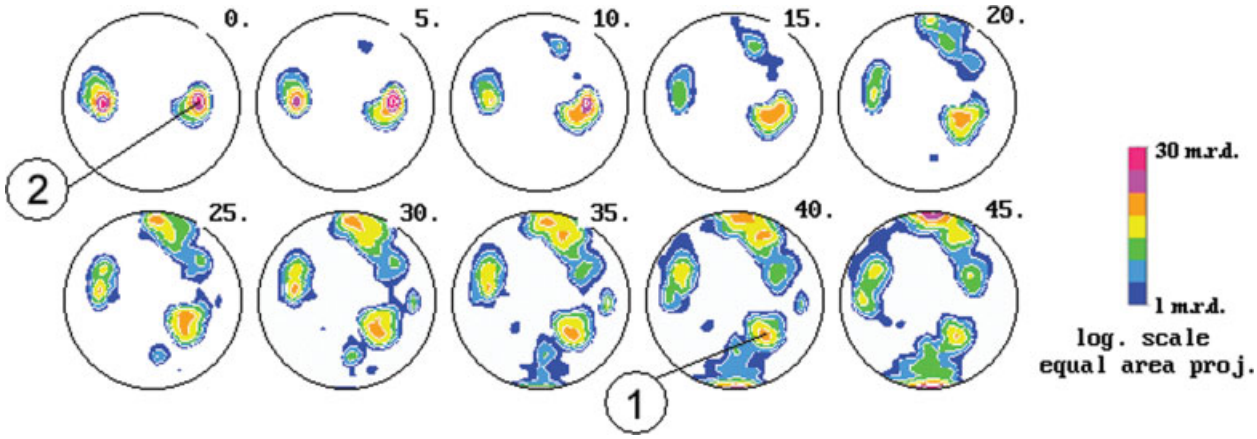

Figure 12. Annealed plate crystal orientation distribution in 5° Euler γ space increments. Note the principal component locations which are labeled 1 and 2. See Table II for quantification of these principal components.

ponent volume. Heat treating at 850°C for 30 min does little to remove the texture; rather it modifies the preferred texture to a {111}⟨123⟩ orientation representing 20% of the component volume. Indeed, a surprising result is that following annealing, the Nitinol tubes have a significantly stronger texture than in the as-drawn condition. In comparison, as-rolled plates have a preferred orientation of {111}⟨112⟩ comprising 15% of the component volume, which changes to a surprising 45% component volume of {435}⟨312⟩ on annealing. In fact, following annealing, the plate exhibited substantial texturing of approximately 75% of the grains which may be due to grain growth and/or recrystallization.

In general, drawn tubes and rolled plates were observed to have few similarities in texture. This implies that for testing and evaluation purposes, Nitinol plate should never be used as a substitute for tubes. Moreover, plates that have been rolled into a cylinder cannot be assumed to have the same texture as actual tubes.

The authors thank Drs. Tom Duerig and Alan Pelton (Nitinol Devices and Components) for their support and for supplying the Nitinol tubing, and Drs. Duerig and Pelton, Dr. Apurva Mehta, Dr. Ekaterina Notkina, Prof. Panos Papadopoulos, and Dr. Youngjean Jung for many helpful discussions and guidance.

References

1. Miyazaki S, Otzuka K, Wayman CM. The shape memory mechanism associated with the martensite transformation in Ti-Ni alloys. I. Self accommodation. Acta Metall 1989;37:1837–1890.
2. Duerig T, Pelton A, Stockel D. An overview of Nitinol medical applications. Mater Sci Eng 1999;A273–275:149–160.
3. Pelton AR, DiCella J, Miyazaki S. Optimization of processing of medical grade Nitinol wire. Min Invas Ther Appl Technol 2000:200-9;107–118.
4. Monasevich LA, Paskal' Yu I, Prib VE, Timonin GD, Chernov DB. Effect of texture on the shape memory effect in titanium nickelide. Met Sci Heat Treat 1979;21:735–737.
5. Li DY, Wu XF, Ko T. The texture of Ti-51.5 at.% Ni rolling plate and its effect on the all-round shape memory effect. Acta Metall Mater 1990;38:19–24.
6. Mulder JH, Thoma PE, Beyer J. Anisotropy of the shape memory effect in tension of cold-rolled 50.8 Ti 49.2 Ni (at. %) sheet. Z Metallkd 1993;1993:501–508.
7. Inoue H, Miwa N, Inakazu N. Texture and shape memory strain in TiNi alloy sheets. Acta Mater 1996;44:4825–4834.
8. Kitamura K, Miyazaki S, Iwai H, Kohl M. Effect of heat-treatment on the texture in rolled Ti-Ni thin plates. Proceedings of the Shape Memory and Superelastic Technologies Conference (SMST-97). Fremont, CA: SMST Society, 1997. p 47–52.
9. Shu YC, Bhattacharya K. The influence of texture on the shape-memory effect in polycrystals. Acta Mater 1998;46:5457–5473.
10. Hornbogen E, Bruckner G, Gottstein G. Microstructure and texture of ausformed NiTi. Z Metallkd 2002;93:3–6.
11. Sitepu H, Schmahl W, Von Dreele B. Use of the generalized spherical-harmonic model for describing texture in polycrystalline NiTi shape memory alloys with time-of-flight neutron diffraction data. Appl Phys A 2002;74:S1676–1678.
12. Gall K, Sehitoglu H. The role of texture in tension-compression asymmetry in polycrystalline NiTi. Int J Plasticity 1999;15:69–92.
13. Vaidyanathan R, Bourke MAM, Dunand DC. Texture, strain, and phase-fraction measurements during mechanical cycling in superelastic NiTi. Metall Mater Trans A 2001;32A:777–786.
14. McNaney JM, Imbeni V, Jung Y, Papadopoulos P, Ritchie RO. An experimental study of the superelastic effect in a shape-memory Nitinol alloy under biaxial loading. Mech Mater 2003;35:969–986.
15. Matthies S, Vinel GW. On the reproduction of the orientation distribution function of textured samples from reduced pole figures using the concept of conditional ghost correction. Phys Stat Sol B 1982;112:K111–K114.
16. Wenk H-R, Matthies S, Donovan J, Chateigner D. BEARTEX, a Windows-based program system for quantitative texture analysis. J Appl Cryst 1998;31:262–269.
17. Kocks UF, Tome CN, Wenk H-R. Texture and anisotropy. New York: Cambridge University Press; 1998. p 195–196.
18. Wenk H-R, Kocks UF. The representation of orientation distributions. Metall Trans 1987;18A:1083–1092.
19. Gao S, Yi S. Experimental study on the anisotropic behavior of textured NiTi pseudoelastic shape memory alloys. Mater Sci Eng 2003;A362:107–111.
20. Yuan WQ, Yi S. Pseudo-elastic strain estimation of textured TiNi shape memory alloys. Mater Sci Eng 1999;A271:439–448.